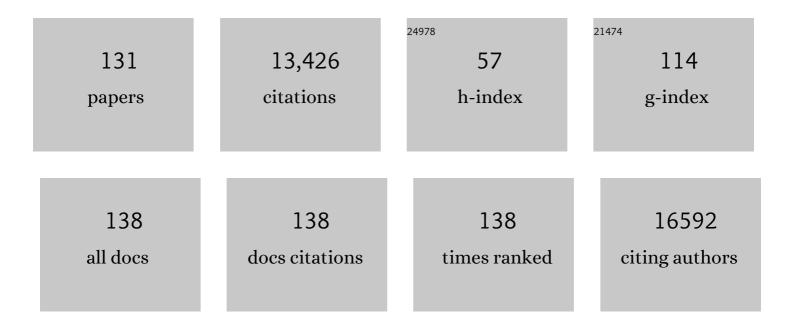
Hyunhyub Ko

List of Publications by Year in descending order

Source: https://exaly.com/author-pdf/8191908/publications.pdf Version: 2024-02-01



#	Article	IF	CITATIONS
1	Nanowire active-matrix circuitry for low-voltage macroscale artificial skin. Nature Materials, 2010, 9, 821-826.	13.3	1,162
2	Nanostructured Surfaces and Assemblies as SERS Media. Small, 2008, 4, 1576-1599.	5.2	726
3	Giant Tunneling Piezoresistance of Composite Elastomers with Interlocked Microdome Arrays for Ultrasensitive and Multimodal Electronic Skins. ACS Nano, 2014, 8, 4689-4697.	7.3	726
4	Fingertip skin–inspired microstructured ferroelectric skins discriminate static/dynamic pressure and temperature stimuli. Science Advances, 2015, 1, e1500661.	4.7	704
5	Tactile-Direction-Sensitive and Stretchable Electronic Skins Based on Human-Skin-Inspired Interlocked Microstructures. ACS Nano, 2014, 8, 12020-12029.	7.3	516
6	Optically- and Thermally-Responsive Programmable Materials Based on Carbon Nanotube-Hydrogel Polymer Composites. Nano Letters, 2011, 11, 3239-3244.	4.5	476
7	Ultrathin compound semiconductor on insulator layers for high-performance nanoscale transistors. Nature, 2010, 468, 286-289.	13.7	373
8	Flexible Ferroelectric Sensors with Ultrahigh Pressure Sensitivity and Linear Response over Exceptionally Broad Pressure Range. ACS Nano, 2018, 12, 4045-4054.	7.3	360
9	Bioinspired Interlocked and Hierarchical Design of ZnO Nanowire Arrays for Static and Dynamic Pressureâ€Sensitive Electronic Skins. Advanced Functional Materials, 2015, 25, 2841-2849.	7.8	315
10	Large-Area Cross-Aligned Silver Nanowire Electrodes for Flexible, Transparent, and Force-Sensitive Mechanochromic Touch Screens. ACS Nano, 2017, 11, 4346-4357.	7.3	287
11	Wearable and flexible sensors for user-interactive health-monitoring devices. Journal of Materials Chemistry B, 2018, 6, 4043-4064.	2.9	255
12	Mimicking Human and Biological Skins for Multifunctional Skin Electronics. Advanced Functional Materials, 2020, 30, 1904523.	7.8	247
13	Triboelectric Generators and Sensors for Self-Powered Wearable Electronics. ACS Nano, 2015, 9, 3421-3427.	7.3	239
14	Metal-catalyzed crystallization of amorphous carbon to graphene. Applied Physics Letters, 2010, 96, .	1.5	234
15	Skin-Inspired Hierarchical Polymer Architectures with Gradient Stiffness for Spacer-Free, Ultrathin, and Highly Sensitive Triboelectric Sensors. ACS Nano, 2018, 12, 3964-3974.	7.3	218
16	Capillary Printing of Highly Aligned Silver Nanowire Transparent Electrodes for High-Performance Optoelectronic Devices. Nano Letters, 2015, 15, 7933-7942.	4.5	196
17	Porous Substrates for Label-Free Molecular Level Detection of Nonresonant Organic Molecules. ACS Nano, 2009, 3, 181-188.	7.3	190
18	Nanoparticleâ€Decorated Nanocanals for Surfaceâ€Enhanced Raman Scattering. Small, 2008, 4, 1980-1984.	5.2	167

#	Article	IF	CITATIONS
19	Octopusâ€Inspired Smart Adhesive Pads for Transfer Printing of Semiconducting Nanomembranes. Advanced Materials, 2016, 28, 7457-7465.	11.1	163
20	Liquid-Crystalline Processing of Highly Oriented Carbon Nanotube Arrays for Thin-Film Transistors. Nano Letters, 2006, 6, 1443-1448.	4.5	157
21	Transparent and conductive nanomembranes with orthogonal silver nanowire arrays for skin-attachable loudspeakers and microphones. Science Advances, 2018, 4, eaas8772.	4.7	155
22	Highly porous graphitic carbon and Ni ₂ P ₂ O ₇ for a high performance aqueous hybrid supercapacitor. Journal of Materials Chemistry A, 2015, 3, 21553-21561.	5.2	153
23	Smart Actuators and Adhesives for Reconfigurable Matter. Accounts of Chemical Research, 2017, 50, 691-702.	7.6	151
24	Tailoring force sensitivity and selectivity by microstructure engineering of multidirectional electronic skins. NPG Asia Materials, 2018, 10, 163-176.	3.8	151
25	Encapsulation of organic active materials in carbon nanotubes for application to high-electrochemical-performance sodium batteries. Energy and Environmental Science, 2016, 9, 1264-1269.	15.6	148
26	An ice-templated, pH-tunable self-assembly route to hierarchically porous graphene nanoscroll networks. Nanoscale, 2014, 6, 9734-9741.	2.8	136
27	Tailoring surface plasmons of high-density gold nanostar assemblies on metal films for surface-enhanced Raman spectroscopy. Nanoscale, 2014, 6, 616-623.	2.8	131
28	Bimetallic Nanocobs: Decorating Silver Nanowires with Gold Nanoparticles. Advanced Materials, 2008, 20, 1544-1549.	11.1	125
29	Carambola-shaped VO ₂ nanostructures: a binder-free air electrode for an aqueous Na–air battery. Journal of Materials Chemistry A, 2017, 5, 2037-2044.	5.2	120
30	Stretchable and wearable colorimetric patches based on thermoresponsive plasmonic microgels embedded in a hydrogel film. NPG Asia Materials, 2018, 10, 912-922.	3.8	120
31	Micro/nanostructured surfaces for self-powered and multifunctional electronic skins. Journal of Materials Chemistry B, 2016, 4, 2999-3018.	2.9	116
32	Nanotube Surface Arrays: Weaving, Bending, and Assembling on Patterned Silicon. Physical Review Letters, 2004, 92, 065502.	2.9	113
33	A Hierarchical Nanoparticleâ€inâ€Micropore Architecture for Enhanced Mechanosensitivity and Stretchability in Mechanochromic Electronic Skins. Advanced Materials, 2019, 31, e1808148.	11.1	113
34	Transparent and Flexible Surface-Enhanced Raman Scattering (SERS) Sensors Based on Gold Nanostar Arrays Embedded in Silicon Rubber Film. ACS Applied Materials & Interfaces, 2017, 9, 44088-44095.	4.0	111
35	Bioinspired Gradient Conductivity and Stiffness for Ultrasensitive Electronic Skins. ACS Nano, 2021, 15, 1795-1804.	7.3	104
36	Biodegradable, electro-active chitin nanofiber films for flexible piezoelectric transducers. Nano Energy, 2018, 48, 275-283.	8.2	101

#	Article	IF	CITATIONS
37	Ultrathin, lightweight and flexible perovskite solar cells with an excellent power-per-weight performance. Journal of Materials Chemistry A, 2019, 7, 1107-1114.	5.2	100
38	Hierarchical urchin-shaped α-MnO2 on graphene-coated carbon microfibers: a binder-free electrode for rechargeable aqueous Na–air battery. NPG Asia Materials, 2016, 8, e294-e294.	3.8	87
39	A superior dye adsorbent towards the hydrogen evolution reaction combining active sites and phase-engineering of (1T/2H) MoS ₂ /α-MoO ₃ hybrid heterostructured nanoflowers. Journal of Materials Chemistry A, 2018, 6, 15320-15329.	5.2	86
40	Redoxâ€Additiveâ€Enhanced High Capacitance Supercapacitors Based on Co ₂ P ₂ O ₇ Nanosheets. Advanced Materials Interfaces, 2017, 4, 1700059.	1.9	85
41	Combing and Bending of Carbon Nanotube Arrays with Confined Microfluidic Flow on Patterned Surfaces. Journal of Physical Chemistry B, 2004, 108, 4385-4393.	1.2	81
42	Sewing machine stitching of polyvinylidene fluoride fibers: programmable textile patterns for wearable triboelectric sensors. Journal of Materials Chemistry A, 2018, 6, 22879-22888.	5.2	80
43	Ferroelectric Multilayer Nanocomposites with Polarization and Stress Concentration Structures for Enhanced Triboelectric Performances. ACS Nano, 2020, 14, 7101-7110.	7.3	79
44	High-Performance Triboelectric Devices via Dielectric Polarization: A Review. Nanoscale Research Letters, 2021, 16, 35.	3.1	79
45	Directed Selfâ€Assembly of Gradient Concentric Carbon Nanotube Rings. Advanced Functional Materials, 2008, 18, 2114-2122.	7.8	77
46	Exploration of cobalt phosphate as a potential catalyst for rechargeable aqueous sodium-air battery. Journal of Power Sources, 2016, 311, 29-34.	4.0	74
47	Soft and ion-conducting hydrogel artificial tongue for astringency perception. Science Advances, 2020, 6, eaba5785.	4.7	74
48	Nanoparticleâ€Enhanced Silverâ€Nanowire Plasmonic Electrodes for Highâ€Performance Organic Optoelectronic Devices. Advanced Materials, 2018, 30, e1800659.	11.1	67
49	Nanoporous Membranes with Mixed Nanoclusters for Raman-Based Label-Free Monitoring of Peroxide Compounds. Analytical Chemistry, 2009, 81, 5740-5748.	3.2	66
50	Broadband omnidirectional light detection in flexible and hierarchical ZnO/Si heterojunction photodiodes. Nano Research, 2017, 10, 22-36.	5.8	66
51	MXene-enhanced Î ² -phase crystallization in ferroelectric porous composites for highly-sensitive dynamic force sensors. Nano Energy, 2021, 89, 106409.	8.2	66
52	Bioenabled Surfaceâ€Mediated Growth of Titania Nanoparticles. Advanced Materials, 2008, 20, 3274-3279.	11.1	64
53	High-Performance MoS ₂ /CuO Nanosheet-on-One-Dimensional Heterojunction Photodetectors. ACS Applied Materials & Interfaces, 2016, 8, 33955-33962.	4.0	64
54	Near-Field Electrospinning for Three-Dimensional Stacked Nanoarchitectures with High Aspect Ratios. Nano Letters, 2020, 20, 441-448.	4.5	64

#	Article	IF	CITATIONS
55	Spatiotemporal Measurement of Arterial Pulse Waves Enabled by Wearable Active-Matrix Pressure Sensor Arrays. ACS Nano, 2022, 16, 368-377.	7.3	63
56	Encapsulating Nanoparticle Arrays into Layer-by-layer Multilayers by Capillary Transfer Lithography. Chemistry of Materials, 2005, 17, 5489-5497.	3.2	62
57	Strain-Sensitive Raman Modes of Carbon Nanotubes in Deflecting Freely Suspended Nanomembranes. Advanced Materials, 2005, 17, 2127-2131.	11.1	61
58	Piezoresistive Tactile Sensor Discriminating Multidirectional Forces. Sensors, 2015, 15, 25463-25473.	2.1	61
59	Hybrid Coreâ^'Shell Nanowire Forests as Self-Selective Chemical Connectors. Nano Letters, 2009, 9, 2054-2058.	4.5	59
60	Self-Healable Reprocessable Triboelectric Nanogenerators Fabricated with Vitrimeric Poly(hindered) Tj ETQq0 0 0	rgBT /Ove	rlock 10 Tf 5

61	Fully stretchable self-charging power unit with micro-supercapacitor and triboelectric nanogenerator based on oxidized single-walled carbon nanotube/polymer electrodes. Nano Energy, 2021, 86, 106083.	8.2	57
62	Particle–Film Plasmons on Periodic Silver Film over Nanosphere (AgFON): A Hybrid Plasmonic Nanoarchitecture for Surface-Enhanced Raman Spectroscopy. ACS Applied Materials & Interfaces, 2016, 8, 634-642.	4.0	56
63	A Fully Biodegradable Ferroelectric Skin Sensor from Edible Porcine Skin Gelatine. Advanced Science, 2021, 8, 2005010.	5.6	56
64	Three-dimensional SnS2 nanopetals for hybrid sodium-air batteries. Electrochimica Acta, 2017, 257, 328-334.	2.6	53
65	Stimuli-responsive micro/nanoporous hairy skin for adaptive thermal insulation and infrared camouflage. Materials Horizons, 2020, 7, 3258-3265.	6.4	53
66	BinaryÂN,S-doped carbon nanospheres from bio-inspired artificial melanosomes: A route to efficient air electrodes for seawater batteries. Journal of Materials Chemistry A, 2018, 6, 24459-24467.	5.2	52
67	Largeâ€Area, Solutionâ€Processed, Hierarchical MAPbI ₃ Nanoribbon Arrays for Selfâ€Powered Flexible Photodetectors. Advanced Optical Materials, 2018, 6, 1800615.	3.6	51
68	Activity-Durability Coincidence of Oxygen Evolution Reaction in the Presence of Carbon Corrosion: Case Study of MnCo ₂ O ₄ Spinel with Carbon Black. ACS Sustainable Chemistry and Engineering, 2018, 6, 9566-9571.	3.2	51
69	Effect of Interfacial Interaction on the Conformational Variation of Poly(vinylidene fluoride) (PVDF) Chains in PVDF/Graphene Oxide (GO) Nanocomposite Fibers and Corresponding Mechanical Properties. ACS Applied Materials & Interfaces, 2019, 11, 13665-13675.	4.0	49
70	Frequency-selective acoustic and haptic smart skin for dual-mode dynamic/static human-machine interface. Science Advances, 2022, 8, eabj9220.	4.7	49
71	Molecular structure engineering of dielectric fluorinated polymers for enhanced performances of triboelectric nanogenerators. Nano Energy, 2018, 53, 37-45.	8.2	47

72 Transfer Printing of Electronic Functions on Arbitrary Complex Surfaces. ACS Nano, 2020, 14, 12-20. 7.3 47

#	Article	IF	CITATIONS
73	Particle-on-Film Gap Plasmons on Antireflective ZnO Nanocone Arrays for Molecular-Level Surface-Enhanced Raman Scattering Sensors. ACS Applied Materials & Interfaces, 2015, 7, 26421-26429.	4.0	45
74	Carbon Nanotube Arrays Encapsulated into Freely Suspended Flexible Films. Chemistry of Materials, 2005, 17, 2490-2493.	3.2	44
75	Flexible Carbonâ€Nanofiber Connectors with Anisotropic Adhesion Properties. Small, 2010, 6, 22-26.	5.2	44
76	Self-powered triboelectric/pyroelectric multimodal sensors with enhanced performances and decoupled multiple stimuli. Nano Energy, 2020, 72, 104671.	8.2	44
77	Ultrasensitive Multimodal Tactile Sensors with Skinâ€Inspired Microstructures through Localized Ferroelectric Polarization. Advanced Science, 2022, 9, e2105423.	5.6	43
78	Nanoscale Semiconductor "X―on Substrate "Y―– Processes, Devices, and Applications. Advanced Materials, 2011, 23, 3115-3127.	11.1	42
79	Boosting the Performance of Organic Optoelectronic Devices Using Multipleâ€Patterned Plasmonic Nanostructures. Advanced Materials, 2016, 28, 4976-4982.	11.1	40
80	Rechargeable Na/Ni batteries based on the Ni(OH) ₂ /NiOOH redox couple with high energy density and good cycling performance. Journal of Materials Chemistry A, 2019, 7, 1564-1573.	5.2	40
81	High-resolution Raman microscopy of curled carbon nanotubes. Applied Physics Letters, 2004, 85, 2598-2600.	1.5	39
82	Directed self-assembly of rhombic carbon nanotube nanomesh films for transparent and stretchable electrodes. Journal of Materials Chemistry C, 2015, 3, 2319-2325.	2.7	39
83	Water-adaptive and repeatable self-healing polymers bearing bulky urea bonds. Polymer Chemistry, 2018, 9, 11-19.	1.9	39
84	Multifunctional, flexible electronic systems based on engineered nanostructured materials. Nanotechnology, 2012, 23, 344001.	1.3	38
85	Tailored Poly(vinylidene fluoride- <i>co</i> -trifluoroethylene) Crystal Orientation for a Triboelectric Nanogenerator through Epitaxial Growth on a Chitin Nanofiber Film. Nano Letters, 2020, 20, 6651-6659.	4.5	38
86	High-Resolution Filtration Patterning of Silver Nanowire Electrodes for Flexible and Transparent Optoelectronic Devices. ACS Applied Materials & amp; Interfaces, 2020, 12, 32154-32162.	4.0	35
87	Polyvinylidene fluoride (PVDF)/cellulose nanocrystal (CNC) nanocomposite fiber and triboelectric textile sensors. Composites Part B: Engineering, 2021, 223, 109098.	5.9	34
88	Freestanding 2D Arrays of Silver Nanorods. Advanced Materials, 2006, 18, 2895-2899.	11.1	32
89	InGaAs Nanomembrane/Si van der Waals Heterojunction Photodiodes with Broadband and High Photoresponsivity. ACS Applied Materials & Interfaces, 2016, 8, 26105-26111.	4.0	32
90	Wet and Dry Adhesion Properties of Self‧elective Nanowire Connectors. Advanced Functional Materials, 2009, 19, 3098-3102.	7.8	31

#	Article	IF	CITATIONS
91	Raman Markers from Silver Nanowire Crossbars. Journal of Physical Chemistry C, 2011, 115, 4387-4394.	1.5	31
92	Feasibility of using hollow double walled Mn2O3 nanocubes for hybrid Na-air battery. Chemical Engineering Journal, 2019, 360, 415-422.	6.6	31
93	Ferroelectricity-Coupled 2D-MXene-Based Hierarchically Designed High-Performance Stretchable Triboelectric Nanogenerator. ACS Nano, 2022, 16, 11415-11427.	7.3	31
94	Hierarchical polymer micropillar arrays decorated with ZnO nanowires. Nanotechnology, 2010, 21, 295305.	1.3	30
95	A Triple-Mode Flexible E-Skin Sensor Interface for Multi-Purpose Wearable Applications. Sensors, 2018, 18, 78.	2.1	30
96	Thermoresponsive Chemical Connectors Based on Hybrid Nanowire Forests. Angewandte Chemie - International Edition, 2010, 49, 616-619.	7.2	29
97	Ultrasensitive Piezoresistive Pressure Sensors Based on Interlocked Micropillar Arrays. BioNanoScience, 2014, 4, 349-355.	1.5	29
98	Hybrid core-multishell nanowire forests for electrical connector applications. Applied Physics Letters, 2009, 94, 263110.	1.5	28
99	Binary Spiky/Spherical Nanoparticle Films with Hierarchical Micro/Nanostructures for High-Performance Flexible Pressure Sensors. ACS Applied Materials & Interfaces, 2020, 12, 58403-58411.	4.0	26
100	Vacuum-Induced Wrinkle Arrays of InGaAs Semiconductor Nanomembranes on Polydimethylsiloxane Microwell Arrays. ACS Nano, 2014, 8, 3080-3087.	7.3	25
101	Solutionâ€Processable, Highâ€Performance Flexible Electroluminescent Devices Based on Highâ€ <i>k</i> Nanodielectrics. Advanced Functional Materials, 2019, 29, 1904377.	7.8	24
102	A high-speed analog-to-digital converter using Josephson self-gating-AND comparators. IEEE Transactions on Magnetics, 1985, 21, 200-203.	1.2	23
103	Highly Stretchable Soundâ€inâ€Display Electronics Based on Strainâ€Insensitive Metallic Nanonetworks. Advanced Science, 2021, 8, 2001647.	5.6	23
104	Flexible high-performance graphene hybrid photodetectors functionalized with gold nanostars and perovskites. NPG Asia Materials, 2020, 12, .	3.8	21
105	A Multi-Functional Physiological Hybrid-Sensing E-Skin Integrated Interface for Wearable IoT Applications. IEEE Transactions on Biomedical Circuits and Systems, 2019, 13, 1535-1544.	2.7	19
106	Electronic Textiles Based on Highly Conducting Poly(vinyl alcohol)/Carbon Nanotube/Silver Nanobelt Hybrid Fibers. ACS Applied Materials & Interfaces, 2021, 13, 31051-31058.	4.0	18
107	Highly Transparent, Flexible, and Self-Healable Thermoacoustic Loudspeakers. ACS Applied Materials & Interfaces, 2020, 12, 53184-53192.	4.0	17
108	Anisotropic silver nanowire dielectric composites for self-healable triboelectric sensors with multi-directional tactile sensitivity. Nano Energy, 2022, 92, 106704.	8.2	16

#	Article	IF	CITATIONS
109	Interdigitated Three-Dimensional Heterogeneous Nanocomposites for High-Performance Mechanochromic Smart Membranes. ACS Nano, 2022, 16, 68-77.	7.3	15
110	A Flexible Highâ€Performance Photoimaging Device Based on Bioinspired Hierarchical Multipleâ€Patterned Plasmonic Nanostructures. Small, 2018, 14, e1703890.	5.2	13
111	High-Performance Hybrid Photovoltaics with Efficient Interfacial Contacts between Vertically Aligned ZnO Nanowire Arrays and Organic Semiconductors. ACS Omega, 2019, 4, 9996-10002.	1.6	13
112	Enhanced thermomechanical property of a self-healing polymer <i>via</i> self-assembly of a reversibly cross-linkable block copolymer. Polymer Chemistry, 2020, 11, 3701-3708.	1.9	13
113	Gate-Controlled Spin-Orbit Interaction in InAs High-Electron Mobility Transistor Layers Epitaxially Transferred onto Si Substrates. ACS Nano, 2013, 7, 9106-9114.	7.3	12
114	Mechanical Properties of Poly(dopamine) oated Graphene Oxide and Poly(vinyl alcohol) Composite Fibers Coated with Reduced Graphene Oxide and Their Use for Piezoresistive Sensing. Particle and Particle Systems Characterization, 2017, 34, 1600382.	1.2	11
115	Engineering crystal phase of Nylon-11 films for ferroelectric device and piezoelectric sensor. Nano Energy, 2021, 88, 106244.	8.2	11
116	Flexible Pyroresistive Graphene Composites for Artificial Thermosensation Differentiating Materials and Solvent Types. ACS Nano, 2022, 16, 1208-1219.	7.3	11
117	Gate-Tunable and Programmable n-InGaAs/Black Phosphorus Heterojunction Diodes. ACS Applied Materials & amp; Interfaces, 2019, 11, 23382-23391.	4.0	10
118	Dynamic and Reprocessable Fluorinated Poly(hindered urea) Network Materials Containing Ionic Liquids to Enhance Triboelectric Performance. ACS Applied Materials & Interfaces, 2022, 14, 17806-17817.	4.0	10
119	pH-tunable plasmonic properties of Ag nanoparticle cores in block copolymer micelle arrays on Ag films. Journal of Materials Chemistry A, 2015, 3, 11730-11735.	5.2	9
120	Large-Area, Highly Sensitive SERS Substrates with Silver Nanowire Thin Films Coated by Microliter-Scale Solution Process. Nanoscale Research Letters, 2017, 12, 581.	3.1	9
121	Highly Stretchable, Conductive Polymer Electrodes with a Mixed AgPdCu and PTFE Network Interlayer for Stretchable Electronics. Advanced Materials Interfaces, 2021, 8, 2001500.	1.9	6
122	Self-healable triboelectric nanogenerators based on ionic poly(hindered urea) network materials cross-linked with fluorinated block copolymers. Polymer Chemistry, 2022, 13, 4343-4351.	1.9	6
123	Spontaneous capillary breakup of suspended gradient polymer stripes into spatially ordered dot arrays. Applied Surface Science, 2019, 475, 1003-1009.	3.1	5
124	Electronic Skin: Bioinspired Interlocked and Hierarchical Design of ZnO Nanowire Arrays for Static and Dynamic Pressure-Sensitive Electronic Skins (Adv. Funct. Mater. 19/2015). Advanced Functional Materials, 2015, 25, 2840-2840.	7.8	4
125	Spin injection and detection in In _{0.53} Ga _{0.47} As nanomembrane channels transferred onto Si substrates. Applied Physics Express, 2014, 7, 093004.	1.1	3
126	Miniaturization of Josephson logic circuits. IEEE Transactions on Magnetics, 1985, 21, 725-728.	1.2	2

#	Article	IF	CITATIONS
127	Surface treatment of MWCNT array and its polymer composites for TIM application. , 2008, , .		1
128	Catalytic effects of zirconium on scratch-healing and mechanical properties of urethane–acrylate automotive clearcoat. Progress in Organic Coatings, 2020, 148, 105813.	1.9	1
129	Inside Front Cover: Directed Selfâ€Assembly of Gradient Concentric Carbon Nanotube Rings (Adv. Funct.) Tj ETÇ	0q1_10.7	84314 rgBT 🜔
130	Lithography-Free Route to Hierarchical Structuring of High-χ Block Copolymers on a Gradient Patterned Surface. Materials, 2020, 13, 304.	1.3	0
131	Stretchable Electroluminescent Devices: Highly Stretchable, Conductive Polymer Electrodes with a Mixed AgPdCu and PTFE Network Interlayer for Stretchable Electronics (Adv. Mater. Interfaces 3/2021). Advanced Materials Interfaces, 2021, 8, 2170015.	1.9	0